arXiv:1404.5008v1 [hep-ph] 20 Apr 2014

Dynamical behavior connection of the gluon distribution and the proton structure function at small-x

G.R.Boroun*

Physics Department, Razi University, Kermanshah 67149, Iran

(Dated: April 22, 2014)

We make a critical study of the relationship between the singlet structure function F_2^S and the gluon distribution $G(x,Q^2)$ proposed in Refs.[4-8], which is frequently used to extract the gluon distribution from the proton structure function. We show that a simple relation is not generally valid in the simplest state. We completed this relation by using a laplace-transform method and hard-Pomeron behavior at LO and NLO at small-x. Our study show that this relation is dependence to the splitting functions and initial conditions at $Q^2 = Q_0^2$ and running coupling constant at NLO. The resulting analytic expression allow us to predict the proton structure function with respect to the gluon distributions and to compare the results with H1 data and a QCD analysis fit. Comparisons with other results are made and predictions for the proposed best approach are also provided.

1.Introduction

The Dokshitzer-Gribov-Lipatov-Altarelli-Parisi (DGLAP) evolution equations [1 − 3] are fundamental tools to study the $\ln Q^2$ and x evolutions of structure functions, where x and Q^2 are Bjorken scaling and the square of the four-vector momentum exchange in deep inelastic scattering (DIS) process respectively. The measurements of the $F_2(x,Q^2)$ structure functions by DIS processes in the small-x region have opened up a new era in parton density measurements inside hadrons. The structure function reflects the momentum distributions of partons in a nucleon. It is also important to know the gluon distribution inside a hadron at small-x because gluons are expected to be dominant in this region. On the other hand, the gluon distribution functions cannot be measured directly through experiments. It is, therefore, important to measure the gluon distribution $G(x,Q^2)$ directly using the proton structure function $F_2(x,Q^2)$. This expectation has led to an approximate phenomenological scheme, as in the past two decades some authors [4-8] reported an ansatz between the gluon distribution function and singlet structure function. The commonly used relation is

$$G(x,Q^2) = K(x)F_2^S(x,Q^2), \tag{1}$$

where $K(x)$ is a parameter to be chosen from the experimental data and those assumed $K(x) = k, ax^b$ or ce^{dx} where k, b, a, c and d are constants. Authors used a Taylor expansion for the gluon and singlet functions at low-x in solving DGLAP evolution equations with applying Eq.1 to the distribution functions. As, Eq.1 is a relationship between singlet structure function and gluon distribution function was proposed in order to facilitate the extraction of the gluon density from the data.

In this paper we deduce the general relations between the proton structure function and the gluon distribution function with analytical methods at leading order (LO) and next-to-leading order (NLO). However, a relation between singlet structure function and gluon distribution function can be determined by simultaneous solutions of coupled DGLAP evolution equations of singlet structure functions and gluon distribution functions. We demonstrate here that the validity of this relation crucially depends on the splitting functions at LO and running coupling constant at NLO. We derive the master equation to extract the relation between the gluon distribution and the proton structure function, by using a Laplace-transform technique at LO and also a hard Pomeron behavior for the gluon distribution up to next-to-leading order (NLO). Our purpose here is to improve the situation with an approximation equation at small-x at LO and NLO. Section 2 outlines the theory and formalism while section 3 is devoted to results and discussions.

2.Compact Formula

The DGLAP evolution equations for the singlet quark structure function and the gluon density have the forms

$$\frac{d}{dlnQ^2}\begin{bmatrix} q(x,Q^2) \\ g(x,Q^2)\end{bmatrix} = \begin{bmatrix} P_{qq} & P_{qg} \\ P_{gq} & P_{gg}\end{bmatrix} \otimes \begin{bmatrix} q(x,Q^2) \\ g(x,Q^2)\end{bmatrix} \tag{2}$$

which emphasized that quark and gluon densities are coupled. The convolution, defined as $P_{ij}\otimes f_j = \int_x^1 \frac{dy}{y} P_{ij}(\frac{x}{y}) f_j(y,Q^2)$, express the possibility that a parton i with momentum fraction x may originate from the

*Electronic address: grboroun@gmail.com; boroun@razi.ac.ir

branching of a parent parton j of the higher momentum fraction y (P_{ij} is the splitting function).
The method of approximate determination a relation between the gluon and structure function is based on the simplification of the convolutions $P_{ij}\otimes f_j$ by the Laplace transforms [9-12] and other methods based on the behavior of the gluon distribution such as the hard Pomeron and the expanding methods [13-15]. Here we present a general solution of the DGLAP evolution equations at low-x, as the gluons are expected to be dominant. Therefore we can neglect the quark singlet part to the evolution equations and also the non-singlet contribution F_2^{NS} can be ignored safely at small-x in the DGLAP equations. Complete solution of the decoupling DGLAP evolution equations for a relation between gluon and singlet functions can be discussed at section 2.2.
The LO DGLAP equations for the singlet and gluon functions can be written as

$$\frac{4\pi}{\alpha_s^{\rm LO}(Q^2)}\frac{\partial F_2^S(x,Q^2)}{\partial \ln Q^2} \simeq 2n_f x\int_x^1 G(z,Q^2)(1-2\frac{x}{z} +2\frac{x^2}{z^2})\frac{dz}{z^2}, \quad (3)$$

and

$$\frac{4\pi}{\alpha_s^{\rm LO}(Q^2)}\frac{\partial G(x,Q^2)}{\partial \ln Q^2}\simeq\frac{33-2n_f}{3}G(x,Q^2) +12G(x,Q^2)\ln\frac{1-x}{x} +12x\int_x^1(\frac{G(z,Q^2)}{z}-\frac{G(x,Q^2)}{x})\frac{dz}{z-x} +12x\int_x^1 G(z,Q^2)(\frac{z}{x}-2+\frac{x}{z}-\frac{x^2}{z^2})\frac{dz}{z^2}. \quad (4)$$

Here $\alpha_s^{\rm LO}(Q^2)$ is given by the LO form

$$\alpha_s^{\rm LO}=\frac{4\pi}{(11-\frac{2}{3}n_f\ln(Q^2/\Lambda^2))}, \quad (5)$$

where n_f being the number of active quark flavors($n_f = 4$) and Λ is the QCD cut-off parameter.

2.1. Laplace Transform method

Authors in Ref.[9-12] uses a somewhat unusual application transforms, in which those first introduce the variable

$$\upsilon \equiv \ln(1/x), \quad (6)$$

into the coupled DGLAP evolution equations, then obtained the coupled equations in the Laplace-space variable s, as we can be written these equations at small-x for our limit

$$\frac{\partial F_2^S}{\partial \ln Q^2}(s,Q^2)\simeq\frac{\alpha_s^{\rm LO}(Q^2)}{4\pi}\Theta_F(s)G(s,Q^2), \quad (7)$$

and

$$\frac{\partial G}{\partial \ln Q^2}(s,Q^2)\simeq\frac{\alpha_s^{\rm LO}(Q^2)}{4\pi}\Phi_G(s)G(s,Q^2), \quad (8)$$

where $F(s) = \mathcal{L}[\hat{F}(\upsilon);s] = \int_0^\infty \hat{F}(\upsilon)e^{-s\upsilon}d\upsilon$ and $G(s) = \mathcal{L}[\hat{G}(\upsilon);s] = \int_0^\infty \hat{G}(\upsilon)e^{-s\upsilon}d\upsilon$ ($\hat{F}(\upsilon)\equiv F(e^{-\upsilon}), \hat{G}(\upsilon)\equiv G(e^{-\upsilon})$). The coefficient functions $\Phi_G(s)$ and $\Theta_F(s)$ are given by [9-12]

$$\Theta_F(s)=2n_f(\frac{1}{1+s}-\frac{2}{2+s}+\frac{2}{3+s}) \quad (9)$$

and

$$\Phi_G(s)=\frac{33-2n_f}{3}+12(\frac{1}{s}-\frac{2}{1+s}-+\frac{1}{2+s} -\frac{1}{3+s}-\psi(1+s)-\gamma_E) \quad (10)$$

where $\psi(x)$ is the digamma function and $\gamma_E = 0.5772156...$ is Euler.s constant.
For obtain an general explicit form between the gluon distribution and the proton structure function at small-x, rewrite Eqs.7 and 8 in s space as

$$\frac{\partial G}{\partial \ln Q^2}(s,Q^2)=\frac{\Phi_G(s)}{\Theta_F(s)}\frac{\partial F_2^S}{\partial \ln Q^2}(s,Q^2). \quad (11)$$

or

$$\frac{\partial G}{\partial \ln Q^2}(s,Q^2)=h(s)\frac{\partial F_2^S}{\partial \ln Q^2}(s,Q^2). \quad (12)$$

In the above equation we used the following property for Laplace transformation

$$\mathcal{L}^{-1}[h(s)\frac{\partial F_2^S(s,Q^2)}{\partial \ln Q^2};\upsilon]=\int_0^\upsilon \frac{\partial \widehat{F_2^S}(w,Q^2)}{\partial \ln Q^2}\widehat{H}(\upsilon-w)dw, \quad (13)$$

where $\widehat{H}(\upsilon)\equiv\mathcal{L}^{-1}[h(s),\upsilon]$. The calculation of $\widehat{H}(\upsilon)$, using Eqs.9 and 10, for LO is straightforward and given by

$$\widehat{H}(\upsilon) = \frac{9}{4}+\frac{13}{8}\,\delta(\upsilon)+\frac{25}{24}\,\delta'(\upsilon) -e^{(\frac{-3}{2}\upsilon)}[\frac{\sqrt{7}}{7}\sin(\frac{\sqrt{7}}{2}\upsilon)+\frac{13}{3}\cos(\frac{\sqrt{7}}{2}\upsilon)]. \quad (14)$$

Here we neglecting the some terms at small-x, as $12\int_0^\upsilon \frac{\partial\widehat{G}}{\partial w}(w,Q^2)\ln(1-e^{-(\upsilon-w)})dw\to 0$. Therefore we obtain an explicit solution for the derivatives of the gluon distribution in terms of the integral

$$\frac{\partial\widehat{G}(\upsilon,Q^2)}{\partial \ln Q^2}=\int_0^\upsilon \frac{\partial\widehat{F}_2^S(w,Q^2)}{\partial \ln Q^2}\widehat{H}(\upsilon-w)dw. \quad (15)$$

Transforming back into x-space, finally we have an approximate approach to the relation between the gluon distribution and singlet structure function at low-x by the following form

$$\begin{aligned} G(x,Q^2) &= G(x,Q_0^2)+\frac{13}{8}\mathcal{FF}(x) \\ &+\frac{9}{4}\int_x^1 \mathcal{FF}(z)\frac{dz}{z}-\frac{25}{24}x\frac{\partial \mathcal{FF}(x)}{\partial x} \\ &-\int_x^1 \mathcal{FF}(z)(\frac{x}{z})^{\frac{3}{2}}(\frac{\sqrt{7}}{7}\sin(\frac{\sqrt{7}}{2}\ln\frac{z}{x}) \\ &+\frac{13}{3}\cos(\frac{\sqrt{7}}{2}\ln\frac{z}{x}))\frac{dz}{z}, \end{aligned} \tag{16}$$

where $\mathcal{FF}(x)\equiv F_2^S(x,Q^2) - F_2^S(x,Q_0^2)$ and $\mathcal{FF}(z)\equiv F_2^S(z,Q^2) - F_2^S(z,Q_0^2)$. Therefore the gluon distribution can be expressed into the singlet structure function by Eq.16 with respect to the initial conditions. This result is general with respect to the approximated limit for the coupled DGLAP evolution equations at small-x, and its the simplest answer to the relation between the gluon distribution and singlet structure function by using a Laplace-transform method.

2.2. Hard-Pomeron behavior

With respect to the Regge-like behavior of the gluon distribution at small-x, we would like to get a simplest formulae to extract the gluon distribution with respect to the proton singlet structure function [13-15]. Authors in Refs.[16-17] shown a simple relation between the gluon and F_2 at small-x based on the coupled integro-differential equations as can be converted in more simple linear relations between the gluon distribution and structure function and its derivatives with respect to $\ln Q^2$. The authors results in Refs.[16-17] are different from Eq.1 as it was proposed in the literature [4-8] to isolate the gluon distribution only with the singlet structure function.

The small-x region of DIS offers a unique possibility to explore the Regge limit of pQCD. This theory is successfully described by the exchange of a particle with appropriate quantum numbers and the exchange particle is called a Regge pole. Phenomenologically, the Regge pole approach to DIS implies that the structure functions are sums of powers in x, modulus logarithmic terms, each with a Q^2- dependent residue factor. This model gives the following parametrization of the DIS structure function $F_2(x,Q^2)$ at small x, $F_2(x,Q^2)=A(Q^2)x^{-\delta}$, that the singlet part of the structure function is controlled by Pomeron exchange at small x. The rapid rise in Q^2 of the structure functions was considered as a sign of departure from the standard Regge behavior. In principle, the HERA data should determine the small-x behavior of the gluon and sea-quark distribution. Roughly speaking, the data on the singlet part of the structure function F_2 constrain the sea quarks and the data on the slope $dF_2/d\ln Q^2$ determine the gluon density. In the DGLAP formalism, the gluon splitting functions are singular as $x\to 0$. Thus, the gluon distribution will become large as $x\to 0$, and its contribution to the evolution of the parton distribution becomes dominant. In particular, the gluon will drive the quark singlet distribution, and, hence, the structure function F_2 becomes large as well, the rise increasing in steepness as Q^2 increases [18-21]. Therefore, the small x limit corresponds to a study of a partonic system inside of a nucleon which is predominantly formed by gluons. This strong rise can eventually violate unitarity and so it has to be tamed by screening effects. However when the density becomes large enough, the gluons start interacting with each others and then their further evolution is non-linear. This happens reduce the growth of gluon distribution and called parton saturation [22-31]. Therefore, the linear evolution equation in this case is modified by non-linear term description gluon recombination. An important point in the gluon saturation approach is the x-dependent saturation scale $Q_s^2(x)$. This scaling argument leads to the conclusion that $\gamma^* p$ cross section, which is a priori function of two independent variable (x and Q^2), is a function of only variable $\tau=\frac{Q^2}{Q_s^2(x)}$ where the saturation scale is given by $Q_s^2(x)=Q_0^2(\frac{x}{x_0})^{-\lambda}$ [32-34] and its known as geometrical scaling. Here Q_0 and x_0 are free parameters and exponent λ is a dynamical quantity of the order $\lambda\sim 0.3$, although one can take into account phenomenologically where exponent λ has an effective Q^2 dependence $\lambda=\lambda_{phn}(Q^2)$. For $Q^2<Q_s^2(x)$ such a scaling is natural, whereas for large $Q^2>Q_s^2(x)$ it is a consequence of hard-poemron behavior from hard diffraction [22-34]. At small x, $Q_s^2(x)\gg\Lambda_{QCD}$ and the approach based on PQCD is fully justified and results are based on the phenomenon of geometric scaling. All results to DIS data from HERA for $x<0.01$ show that geometrical scaling was found in the data from different experiments. In the limit of high energy, PQCD consistently predicts that the high gluon density should form a Color Glass Condensate (CGC), where the interaction probability in DIS becomes large and this is characterized by a hard saturation scale $Q_s(x)$ which grows rapidity with $1/x$ [22-31]. In this region, the nonlinear saturation dynamics is incorporated into the CGC model. As, it is valid only for Q^2 less than or of the order of the saturation momentum, which is at most several GeV^2, while the fit result to SGK [25] model extends up to Q^2 of the order of several hundred GeV^2. Indeed, the extended scaling at $Q^2>Q_s^2$ arises from the general non-linear evolution equations in the kinematical range. The validity of these evolution equations in the present of saturation has been estimated as $Q_s^2(x)<Q^2<Q_s^4(x)/\Lambda_{QCD}^2$. This means that the geometric scal-

ing for all momenta Q^2 have to satisfied this inequality as, $\ln(Q^2/Q_s^2) \ll \ln(Q_s^2/\Lambda_{QCD}^2)$. At soft momenta $Q^2 \leq Q_s^2$ this scaling is an expected consequence of saturation and at high momenta $1 < \ln(Q^2/Q_s^2) \ll \ln(Q_s^2/\Lambda_{QCD}^2)$ it rather corresponds to a regime where parton densities are small, and linear evolution equations apply.
The overall physical picture is dependence to the different regions in the (x, Q^2)-plane. For $Q^2 < Q_s^2(x)$ the linear evolution is strongly perturbed by nonlinear effects where the parton system becomes dense and the saturation corrections start to play an important role. In this region the dipole cross section is bounded by an energy independent value, as the dipole cross section was proposed [22-31] to have the form $\sigma_{dipole}(x,r) = \sigma_0\{1 - exp(-r^2 Q_s^2(x)/4)\}$ which impose the unitarity condition ($\sigma_{q\overline{q}} \leq \sigma_0$) for large dipole sizes r. At small -r region, the dipole cross section is related to the gluon density where it is valid in the double logarithmic approximation. This geometrical scaling holds until the line boundary where $Q^2 = Q_s^2(x)$. As the gluon density is $xg(x, Q^2 = Q_s^2(x)) = r^0 x^{-\lambda}$, and the parameter r_0 specifies the normalization along the critical line. Thus, the saturation scale is an intrinsic characteristic of a dense gluon system. For $Q^2 > Q_s^2(x)$ the nonlinear screening effects can be neglected and evolution of parton densities is governed by the linear DGLAP equations [35-37]. Therefore, the validity of our method only holds in the kinematic region $Q^2 \gg Q_s^3/\Lambda_{QCD}$. Hence, as x gets smaller, the gluon distribution grows rapidly and $\lambda \to \delta$ where δ is the hard pomeron exponent. So, the dipole cross section extracted from DIS data with assuming a hard pomeron dependence, as $\sigma \sim x^{-\delta}$. Therefore we study the DGLAP evolution upon the geometrical scaling in the region $Q^2 > Q_s^2(x)$ with solving the linear DGLAP evolution equation starting from the gluon distribution satisfying the hard-pomeron behavior. The gluon distribution at small-x increase with decreasing x as

$$G(x, Q^2) = f(Q^2) x^{-\delta}. \tag{17}$$

The form $x^{-\delta}$ of the gluon parameterization at small x is suggested by Regge behavior, but because the conventional Regge exchange is that of a soft Pomeron, with $\delta \sim 0$, we may also allow a hard Pomeron with $\delta \sim 0.5$ [18-21]. Based on the hard Pomeron behavior for the gluon distribution, let us put Eq.(17) in Eqs.3 and 4. Let us introduce the variable $y = \frac{x}{z}$. After doing the integration over y , Eqs.3 and 4 can be rewritten as

$$\frac{4\pi}{\alpha_s^{\rm LO}(Q^2)} \frac{\partial F_2^S(x,Q^2)}{\partial \ln Q^2} \simeq 2n_f G(x,Q^2) \times \int_x^1 z^\delta (1 - 2y + 2y^2) dy, \tag{18}$$

and

$$\frac{4\pi}{\alpha_s^{\rm LO}(Q^2)} \frac{\partial G(x,Q^2)}{\partial \ln Q^2} \simeq \frac{33 - 2n_f}{3} G(x,Q^2) + 12 G(x,Q^2) \ln \frac{1-x}{x} + 12 G(x,Q^2) \int_x^1 (y^{1+\delta} - 1) \frac{dy}{y(1-y)} + 12 G(x,Q^2) \int_x^1 y^\delta (y^{-1} - 2 + y - y^2) dy. \tag{19}$$

Consequently

$$\frac{\partial G(x,Q^2)}{\partial \ln Q^2} = \frac{g1}{p1} \frac{\partial F_2^S(x,Q^2)}{\partial \ln Q^2}, \tag{20}$$

where

$$p_1 = 2n_f \int_x^1 z^\delta (1 - 2y + 2y^2) dy, \tag{21}$$

and

$$g_1 = \frac{33 - 2n_f}{3} + 12 \ln \frac{1-x}{x} + 12 \int_x^1 (y^{1+\delta} - 1) \frac{dy}{y(1-y)} + 12 \int_x^1 y^\delta (\frac{1}{y} - 2 + y - y^2) dy. \tag{22}$$

Eq.20 is independent of the running coupling constant ($\alpha_s(Q^2)$) at LO. After successive integrations of both sides of Eq.20, and some rearranging, we find an simplest equation which determine $G(x, Q^2)$ in terms of $F_2^S(x, Q^2)$. Consequently

$$G(x,Q^2) = \frac{g_1}{p_1} F_2^S(x,Q^2) + [G(x,Q_0^2) - \frac{g_1}{p_1} F_2^S(x,Q_0^2)]. \tag{23}$$

We observe that this equation demonstrates the close relation between $G(x, Q^2)$ and $F_2^S(x, Q^2)$ at small-x into the initial conditions at Q_0^2 at LO by using a hard-Pomeron behavior for the gluon distribution.
The NLO corrections are add to LO, as the splitting functions $P_{ij}^{,}s$ are the LO and NLO Altarelli- Parisi splitting kernels by the following form

$$P_{ij}(x, \alpha_s(Q^2)) = P_{ij}^{\rm LO}(x) + \frac{\alpha_s(Q^2)}{2\pi} P_{ij}^{\rm NLO}(x). \tag{24}$$

The next-to-leading order is the standard approximation for most important processes. The corresponding one- and two-loop splitting functions have been known for a long time. Also, the NNLO corrections can be need to be included, in order to obtain a quantitatively reliable predictions for hard processes at present and future high-energy colliders [38].

The running coupling constant $\frac{\alpha_s}{2\pi}$ has the form in the LO and NLO respectively

$$\frac{\alpha_s^{\rm LO}}{2\pi} = \frac{2}{\beta_0 \ln \frac{Q^2}{\Lambda^2}}, \tag{25}$$

and

$$\frac{\alpha_s^{\rm NLO}}{2\pi} = \frac{2}{\beta_0 \ln \frac{Q^2}{\Lambda^2}}[1 - \frac{\beta_1 \ln \ln \frac{Q^2}{\Lambda^2}}{\beta_0^2 \ln \frac{Q^2}{\Lambda^2}}], \tag{26}$$

where $\beta_0 = \frac{1}{3}(33-2N_f)$ and $\beta_1 = 102 - \frac{38}{3}N_f$ are the one-loop and two-loop corrections to the QCD β-function. Therefore the DGLAP evolution equations have these behavior at NLO with respect to the hard-Pomeron behavior at small-x, as we have

$$\frac{dG(x,Q^2)}{d\ln Q^2} = \frac{\alpha_s}{4\pi}[g_1 + (\frac{\alpha_s}{4\pi})g_2]G(x,Q^2), \tag{27}$$

and

$$\frac{dF_2^S(x,Q^2)}{d\ln Q^2} = \frac{\alpha_s}{4\pi}[p_1 + (\frac{\alpha_s}{4\pi})p_2]G(x,Q^2), \tag{28}$$

where

$$\begin{aligned} g_2 \;=\; & 2\frac{(12C_F n_f T_R - 46 C_A n_f T_R)}{9\delta}(1-x^\delta) \\ & +2[n_f T_R(\frac{-61}{9}C_F + \frac{172}{72}C_A) + C_A^2(\frac{1643}{54} - \frac{22}{3}\zeta(2) \\ & -8\zeta(3))]\frac{1-x^{1+\delta}}{1+\delta}, \end{aligned} \tag{29}$$

and

$$p_2 = \frac{\alpha_s}{4\pi}\frac{80 C_A N_f T_R}{9\delta}(1-x^\delta), \tag{30}$$

where p_2 is the NLO kernel after doing the integration based on the hard Pomeron behavior at Eq.28 according to the NLO splitting function in Appendix. Therefore the close relation between the gluon distribution and singlet structure functions at NLO, when the coupling is fixed, is given by

$$G(x,Q^2) = kF_2^S(x,Q^2) + [G(x,Q_0^2) - kF_2^S(x,Q_0^2)], \tag{31}$$

where

$$k = \frac{g_1 + \frac{\alpha_s}{4\pi}g_2}{p_1 + \frac{\alpha_s}{4\pi}p_2}. \tag{32}$$

We now pass to the more realistic case with running coupling. In this case the relation between the distribution functions takes the form

$$G(x,Q^2) = G(x,Q_0^2) + \int_{Q_0^2}^{Q^2} k\frac{\partial F_2^S(x,Q^2)}{\partial \ln Q^2} d\ln Q^2. \tag{33}$$

Similarly, We get the singlet structure function evolution at NLO, as

$$F_2^S(x,Q^2) = F_2^S(x,Q_0^2) + \int_{Q_0^2}^{Q^2} k'\frac{\partial G(x,Q^2)}{\partial \ln Q^2} d\ln Q^2, \tag{34}$$

where

$$k' = \frac{p_1 + \frac{\alpha_s}{4\pi}p_2}{g_1 + \frac{\alpha_s}{4\pi}g_2}. \tag{35}$$

The expansion of the results from NLO to NNLO approximation can be done easily. Here we used our approximation approach to obtained a simplest relation between the gluon distribution and singlet structure function. The complete calculation of the DGLAP evolution equations, when the singlet quark distribution is essentially driven by the generic instability of the gluon distribution, can be down numerically for shown that what is the best relation between the distribution functions at LO up to NNLO. In a resent paper [38] the distribution functions have been obtained by solving decoupling DGLAP evolution equations at LO up to NNLO with respect to the hard pomeron behavior for the parton distributions at low-x. So in the next section we try to do this comparison for the distribution functions using available results at NNLO. Eqs.16, 23 and 31-34 are our results for connection between the gluon distribution and singlet structure function at small-x by using the Laplace-transform and the hard-Pomeron behavior (LO up to NLO) respectively. Therefore we show that Eq.1 is not generally true and its validity crucially depends on the splitting functions and the initial conditions.

3.Results and Discussions

In order to show our results we computed the gluon distribution function on the l.h.s of formulas (16, 23 and 31) at small-x with respect to the initial conditions according to the Block distribution [9-12,39-40]. This distribution represent the spectrum of possible behavior of the proton structure function and gluon distribution in the region $x > 0.00001$ and $0.11 \leq Q^2 \leq 1200 GeV^2$. We begin by illustration the use of the analytical expression in Eq.16 to derive $G(x,Q^2)$ from $F_2^{\gamma p}(x,Q^2)$ in the case of Refs.[9-12,39-40]. We take the published initial distributions as our basic input at $Q_0^2 = 1 GeV^2$, and use this distribution to calculate the proton structure function needed in $\mathcal{FF}(x)$. Then, we solve Eq.16 for the gluon distribution by this $F_2^{\gamma p}(x,Q^2)$ and compared the results with the published gluon distributions. In Fig.1 we show the LO x-space results for the gluon distribution for two representative values of Q^2. The curves are the published Block [9-12] gluon distribution,

Donnachie and Landshoff (DL) [18-21], GRV-HO [41-42] and GJR parameterization [43].
In Fig.2 we present results for the gluon distribution at LO and NLO using the hard-Pomeron behavior for the gluon distribution function. This seems to indicate that the gluon distribution is dominated at small-x by hard-Pomeron exchange. This powerful approach to the small-x data for $G(x,Q^2)$ extends the Regge phenomenology that is so successful for hadronic processes. The hard intercept is $\delta = 0.437$ and we choose Λ such that $\alpha_s(M_Z^2) = 0.116$, this gives $\Lambda^{NLO}_{n_f=4} = 400MeV$ [19-21]. We compared our results by published Block [9-12] gluon distribution, Donnachie and Landshoff (DL) [18-21], GRV-HO [41-42] and GJR parameterization [43]. As can be seen, the values of the gluon distribution function increase as x decreases. This is because the hard-Pomeron exchange defined by DL model is expected to hold in the small-x limit. Comparing our results in Figs.1 and 2 with other results indicates that our global solution (Eq.16) and hard-Pomeron solution (Eqs.23, 31) at the simplest case are compatible with other phenomenological models and this is the reason why the approximate relation (1) is not valid at small-x. In order to compare our results with the experimental data, using Eq.34 for the evolution of the proton structure function with respect to the gluon distribution function. We show a plot of the proton structure function in Fig.3 for values of $Q^2 = 8.5\ GeV^2$ and 20 GeV^2, compared to the values measured by the H1 collaboration [45-46] and a QCD fit based on ZEUS data [39-40]. For each Q^2, there is a cross-over point for both the curves where both the predictions are numerically equal. As we wants to have a good comparison between our results and others, we have to include the singlet distribution functions in DGLAP evolution equations. However, as there is yet no such simple relation between the singlet structure function and gluon distribution at LO up to NNLO, we rather appeal to the numerical results of Ref.[38]. In Fig.4 we show the ratio $\frac{G(x,Q^2)}{F_2^S(x,Q^2)}$ at $Q^2 = 20GeV^2$. In this figure we show that this ratio is hardly negligible. In order to have more accurate solution for the proton structure function, we need to a best global fit for this ratio, using NNLO analysis data in Fig.4. We compared our results for the proton structure function at NNLO with H1 data [45-46] and GJR parameterization [43] and also the gluon distribution function at $Q^2 = 20GeV^2$ in Fig.5. It is clear from this figure for F_2 and G that our results, at NNLO analysis and considering of the singlet parton distribution, are comparable with other results.
In conclusion, the simple relation (1) between the gluon distribution and singlet structure function is not generally valid at small-x. We show that the gluon distribution can be estimated with respect to the splitting functions and initial conditions in a general model by using a Laplace-transform method and hard-Pomeron model at LO and NLO. Therefore our results at simplest approach lead to different results from those at Refs.[4-8]. Further, we need the singlet structure function at the DGLAP evolution equations for the numerical relation between the gluon distribution and single structure function. Moreover we proposed one general numerical approach at NNLO for this connection and conclude that this numerical approach is agreeing with others results.

Acknowledgements Author would like to thank the anonymous referee of the paper for his/her careful reading of the manuscript and for the productive discussions.

Appendix

The NLO splitting function for the singlet structure function is as follows

$$\begin{aligned} p^2_{qg} &= 2C_F N_f T_R\{4-9x-(1-4x)\ln x-(1-2x)\ln^2 x \\ &+4\ln(1-x)+[2\ln^2(\frac{1-x}{x})-4\ln(\frac{1-x}{x})-\frac{2}{3}\pi^2 \\ &+10]P_{qg}(x)\}+2C_A N_f T_R\{\frac{182}{9}+\frac{14}{9}x+\frac{40}{9x} \\ &+(\frac{136}{3}x-\frac{38}{3})\ln x-4\ln(1-x)-(2+8x)\ln\ln^2 x \\ &+2P_{qg}(-x)S_2(x)+[-\ln^2 x+\frac{44}{3}\ln x-2\ln^2(1-x) \\ &+4\ln(1-x)+\frac{\pi^2}{3}-\frac{218}{9}]P_{qg}(x)\} \end{aligned} \tag{36}$$

where $P_{qg}(x) = x^2+(1-x)^2$ and $S_2(x) = \int_{\frac{x}{1+x}}^{\frac{1}{1+x}} \frac{dz}{z}\ln(\frac{1-z}{z})$. The small-$x$ limit of the NLO splitting function for the evolution of the singlet quark is then [44]

$$p^2_{qg} \longrightarrow \frac{\alpha_s}{4\pi}\frac{80C_A N_f T_R}{9x}. \tag{37}$$

where the casimir operators of colour SU(3) are defined as $C_A = 3,\ C_F = \frac{4}{3}$ and $T_R = \frac{1}{2}$.

REFERENCES

1. Yu.L.Dokshitzer, Sov.Phys.JETP **46**, 641(1977).
2. G.Altarelli and G.Parisi, Nucl.Phys.B **126**, 298(1977).
3. V.N.Gribov and L.N.Lipatov, Sov.J.Nucl.Phys. **15**, 438(1972).
4. J.K.Sarma and B.Das, Phys.Lett.B **304**, 323(1993).
5. J.K.Sarma, D.K.Choudhury and G.K.Medhi, Phys.Lett.B **403**, 139(1997).
6. R.Baishya and J.K.Sarma, Phys.Rev.D **74**,

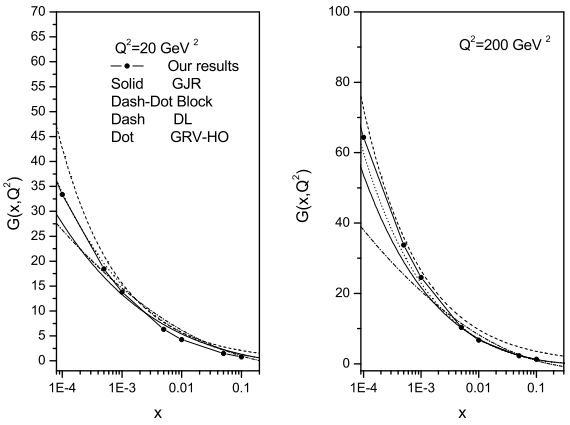

FIG. 1: The gluon distribution, $G(x,Q^2)$, for $Q^2 = 20$ and $200GeV^2$ by using a Laplace-transform. Our results compared to the Block model [9-12], DL model [18-21], GRV-HO parameterization [41-42] and GJR parameterization [43].

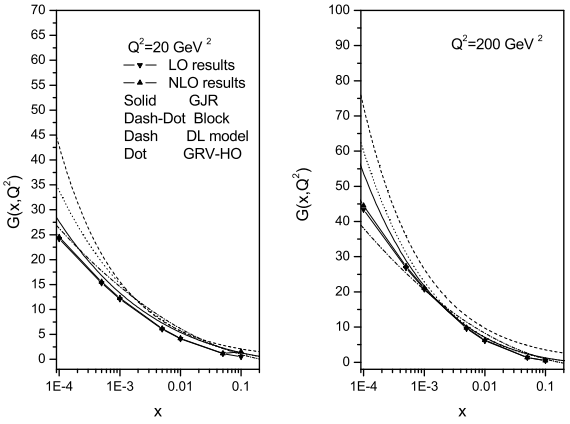

FIG. 2: The same as Fig.1 but for a hard-Pomeron behavior at LO and NLO.

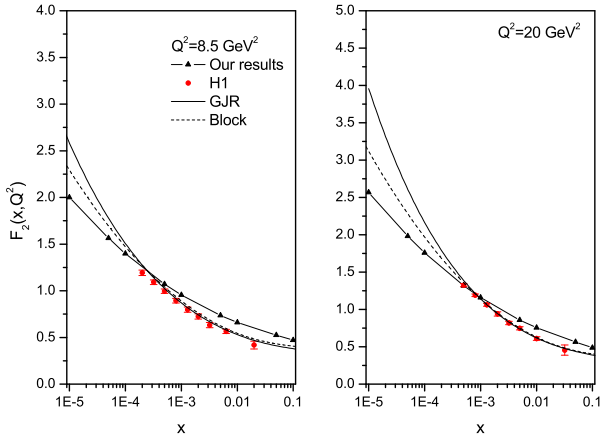

FIG. 3: The proton structure function, $F_2(x,Q^2)$, for $Q^2 = 8.5$ and $20GeV^2$ with respect to a hard-pomeron behavior. Our results compared to the Block model [9-12], GJR parameterization [43] and H1 data [45-46].

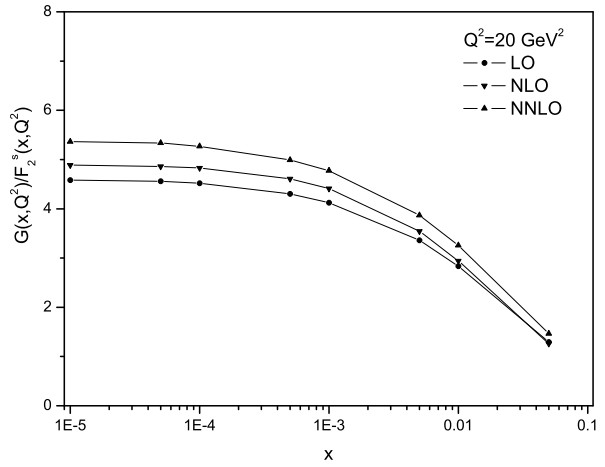

FIG. 4: The ratio $\frac{G(x,Q^2)}{F_2^S(x,Q^2)}$ at LO up to NNLO when we consider the complete form of the DGLAP evolution equations.

107702(2006).
7. R.Baishya, U.Jamil and J.K.Sarma, Phys.Rev.D **79**, 034030(2009).
8. M.Devee, R.Baishya and J.K.Sarma, Eur.Phys.J.C **72**, 2036(2012).
9. M.M.Block, L.Durand, D.W.McKay, Phys.Rev.D**77**, 094003(2008).
10. M.M.Block, L.Durand, D.W.McKay, Phys.Rev.D**79**, 014031(2009).
11. M.M.Block, Eur.Phys.J.C**65**, 1(2010).
12. M.M.Block, L.Durand, P.Ha and D.W.McKay, Phys.Rev.D**83**, 054009(2011).
13. G.R.Boroun, JETP**106**, 700(2008).
14. G.R.Boroun and B.Rezaei, Eur.Phys.J.C**72**, 2221(2012).
15. B.Rezaei and G.R.Boroun, JETP**112**, 381(2011).
16. A.V.Kotikov, Phys.Rev.D **49**, 5746(1994).
17. A.V.Kotikov and G.Parente, Phys.Lett.B **379**, 195(1996).
18. A.Donnachie and P.V.Landshoff, Phys.Lett.B **437**, 408(1998).
19. A.Donnachie and P.V.Landshoff, Phys.Lett.B **550**, 160(2002).
20. P.V.Landshoff, arXiv:hep-ph/0203084 (2002).
21. P.V.Landshoff, arXiv:hep-ph/0209364 (2002).
22. K.Golec-Biernat, J.Phys.G **28**, 1057(2002).
23. K.Golec-Biernat, Acta Phys.Pol.B **35**, 3103(2004).
24. K.Golec-Biernat, Acta Phys.Pol.B **33**, 2771(2002).

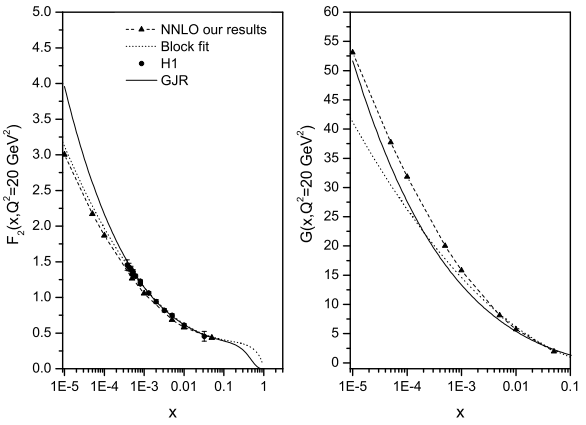

FIG. 5: Numerical estimates at $Q^2 = 20\ GeV^2$, for the proton structure function and gluon distribution function at NNLO analysis and at the complete form of the DGLAP evolution equations, compared with other results.

25. A.M.Stato, K.Golec-Biernat and J.Kwiecinski, Phys.Rev.Lett.**86**, 596(2001).
26. E.Iancu, K.Itakura and S.Munier, Phys.Lett.B **590**, 199(2004).
27. E.Iancu, K.Itakura and S.Munier, Nucl.Phys.A **708**, 327(2002).
28. L. McLerran and R. Venugopalan, Phys.Rev.D**49**, 2233(1994).
29. E. Iancu, A. Leonidov and L. McLerran, Nucl.Phys.A**692**, 583(2001).
30. E. Iancu, A. Leonidov and L. McLerran, Phys.Lett.B**510**, 133(2001).
31. E. Ferreiro, E. Iancu, A. Leonidov and L. McLerran, Nucl.Phys.A**703**, 489(2002).
32. M.Praszalowicz and T.Stebel, arXiv:hep-ph/1302.4227(2013).
33. G.Beuf and D.Royon, arXiv:hep-ph/0810.5082(2008).
34. M.Praszalowicz, arXiv:hep-ph/1304.1867(2013).
35. J.R.Forshaw and G.Shaw, JHEP**12**, 052(2004).
36. J.Kwiecinski and A.M.Stasto, Phys.Rev.D.**66**, 014013(2002).
37. F.Caola and S.Forte, Phys.Rev.Lett.**101**, 022001(2008).
38. G.R.Boroun and B.Rezaei, Eur.Phys.J.C**73**, 2412(2013).
39. M.M.Block, E.L.Berger, C-I Tan, Phys.Rev.Lett**97**, 252003(2006).
40. E.L.Berger, M.M.Block, C-I Tan, Phys.Rev.Lett**98**, 242001(2007).
41. M.Gluk, E.Reya and A.Voget, Z.Phys.C**67**, 433(1995).
42. M.Gluk, E.Reya and A.Voget, Eur.Phys.J.C**5**, 461(1998).
43. M. Gluck, P. Jimenez-Delgado, E. Reya, Eur.Phys.J.C **53**, 355(2008).
44. R.K.Ellis , W.J.Stirling and B.R.Webber, *QCD and Collider Physics*(Cambridge University Press)1996.
45. $H1$ Collab., C.Adloff *et al.*, Eur.Phys.J.C **21**, 33(2001).
46. $H1$ Collab., C.Adloff *et al.*, Eur.Phys.J.C **71**, 1579(2011).